GHGT-12

Does numerical modelling of the onset of dissolution-convection reliably reproduce this key stabilization process in CO_2 Storage?

Hayley Vosper*, Karen Kirk, Chris Rochelle, Dave Noy and Andy Chadwick

Britsh Geological Survey, Keyworth, Nottingham, NG12 5GG

Abstract

Dissolution of carbon dioxide into water is a key medium-term CO_2 plume stabilization process. It proceeds much more quickly when aided by convection than when driven by diffusion alone. The onset of the convection process is not well understood, so laboratory experiments using a Hele-Shaw cell containing a porous medium were used to reproduce the process of CO_2 dissolution and convection in water. High resolution numerical flow models were then used to replicate the laboratory results. They show a remarkably good match in terms of convective plume temporal and spatial development. This suggests that numerical models of dissolution-convection at much larger reservoir scales can reliably predict the onset of dissolution-convection.

Peer-review under responsibility of the Organizing Committee of GHGT-12

Keywords: CO2 Storage, Convection, Hele-Shaw, Dissolution, Storage Security, Stabilization.

1. Introduction

The long-term trapping of carbon dioxide (CO_2) within deep geological storage reservoirs is dependent upon CO_2 - water - rock geochemical reactions that will trap buoyant, dense phase CO_2 as less mobile forms. Dissolution is perhaps the key initial stabilization process because it converts buoyantly trapped free CO_2 into a gravitationally stable dissolved state. Crucially it acts on decadal through to millennial time-scales, much faster than mineralization processes. Initial dissolution is driven by molecular diffusion followed at some point in time by density-driven convective mixing of dissolved CO_2 in the aquifer brine (brine rich in CO_2 being denser than that without CO_2).

* Corresponding author. Tel.: +44-(0)115-936-3463.
  E-mail address: hayleyv@bgs.ac.uk

Diffusion is a slow process, which by itself cannot remove large amounts of buoyant free CO_2 from the system, whereas convective mixing allows free CO_2 to be exposed to CO_2-undersaturated brine and is crucial to dissolving the large amounts of CO_2 required for significant stabilization to occur.

The transition from a stable near-horizontal diffusion-driven interface between the buoyant CO_2 and the underlying aquifer brine, to an unstable state in which plumes of denser CO_2-saturated brine start to sink, marks the onset of convection. Perturbations from the horizontal interface are required for plume formation and in physical experiments natural variations and heterogeneity provide the triggers. Numerical flow simulations at reservoir scales suggest that convection might start as early as a few months after initiation of dissolution, but this is poorly-constrained and often depends on numerical rounding errors in the computation, which have no geological basis, to trigger the instabilities. Other authors have used random permeability distributions to capture the effects of heterogeneity in plume formation [1, 2].

The objective of this paper is to reproduce the onset of dissolution-convection in a porous medium in the laboratory, and then to test whether a high-resolution flow simulation of the experiment can reliably reproduce the real-world observations.

To visualize the descending plumes of dissolved CO_2 on a laboratory scale, a Hele-Shaw cell with a porous medium was constructed (Section 2). Numerical simulations of the laboratory experiment were run using TOUGH2 software for both a homogeneous model where plume formation is triggered by numerical errors and a heterogeneous model with a random permeability distribution (Section 3). Experimental and numerical results are compared in Section 4.

2. Experimental

Previous experimental work [3, 4] has demonstrated that diffusion-convection processes do occur and qualitative comparisons have been made with numerical flow models. In this study we focus specifically on the transition from pure diffusion to convection and the very early stage of convective plume development. We set up a Hele-Shaw cell filled with transparent glass beads to create a porous medium and observed the transition from a stable diffusion-driven interface to convective plume formation.

The Hele-Shaw cell comprised two matched glass sheets 65 cm wide and 36 cm high, separated by a cavity of 1.1 mm spacing, filled with glass beads 0.4 – 0.6 mm in diameter, and water. (Simple filling of the cavity by pouring in the beads produces high permeability artefacts at the glass surface. To avoid this, the beads were glued to the glass sheets using a clear liquid waterproof sealant, and the glass sheets pressed together and sealed around the edges whilst the sealant was still flexible, to allow close packing of the beads). A pH colour-sensitive reagent was added to the water to identify where CO_2 had acidified the water, and care was taken to ensure the expulsion of all air bubbles. CO_2 was introduced into a small air gap at the top of the cell after being pumped through water to ensure it was saturated with water vapour. Time-lapse photography was used to track the experimental results, capturing an image every minute. Initially the water is displayed as purple and presence of CO_2 is indicated in yellow.

Within a few minutes a thin planar layer of reduced pH CO_2-saturated water formed at the top of the cell (Fig. 1). Subsequently, instabilities started to form and after about fifteen minutes these became discernible as discrete plumes of descending CO_2-charged water. The plumes continued to travel vertically down and approached the bottom of the cell after 8 hours.

Photographs of the Hele-Shaw cell after 30, 60, 120 and 240 minutes of CO_2 injected into the top of the cell show distinct plumes forming and growing with time as dissolved CO_2 propagates downwards through the cell and convection enhances the fluid mixing (Fig. 1). At later times the plumes begin to form lobes and break up and the edges become hazy as CO_2 in the plumes mixes in the surrounding water through diffusion processes. Much greater concentrations of CO_2 are revealed at the edges of the cell than in the middle. This effect is clearly artificial and related to the width of the cell where preferential pathways exist at the edges. The results in the centre of the cell are clear and show similar plumes to other experiments [3, 4] and are used for analysis (Section 4).
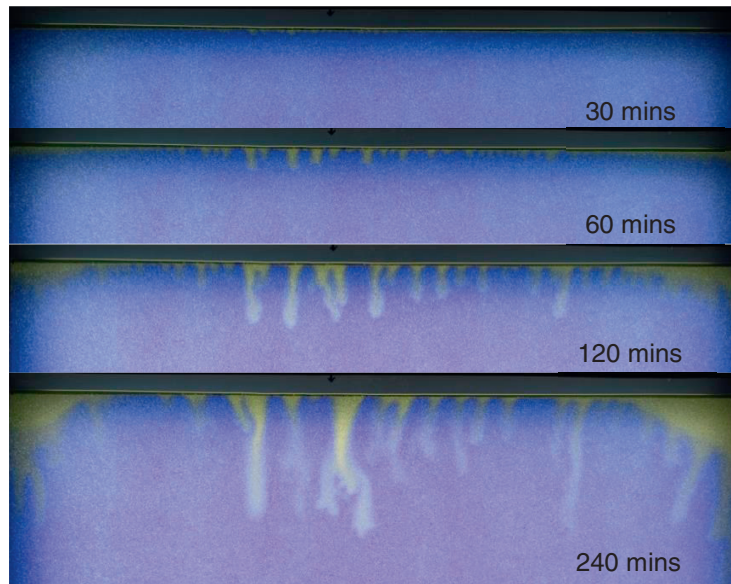
Fig. 1: Snapshots of the Hele-Shaw cell after 30, 60, 120 and 240 minutes.

The length of each of plume was measured (Fig. 2) from its base to the tip and the spacing defined as the distance between the midpoints of adjacent plumes. This definition of spacing is used to represent the wavelength of the plumes. The width of each plume is more subjective and difficult to measure, particularly at early times when the plumes are closely packed with hazy edges and also at later times when the width varies considerably along the length of the plume. There is a black band (Fig. 2) level with the top of the arrows depicting the plume length. The water level actually reaches up to the top of the yellow line in the photographs and the black line is a photographic artefact and not representative of any physical phenomenon. The plume length is therefore measured from the base of the yellow line as a reference point for consistency with all the photographs.
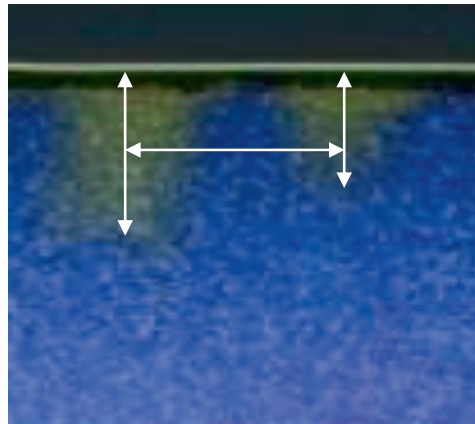

Fig. 2: The measurement technique for length and spacing (wavelength) of the plumes

The length of all the plumes was measured at early times and the maximum length recorded at each time (Fig. 3). The maximum plume length increased linearly with time at a rate of 0.5 mm/minute until interaction with the bottom of the cell became significant. Extrapolating the linear relationship back to the x-axis gives an estimate for the onset time (the time at which plumes begin to grow) as 20 minutes. Plumes were actually first observed in the photographs at around 15 minutes, but were difficult to measure. Taking the average plume length, rather than the

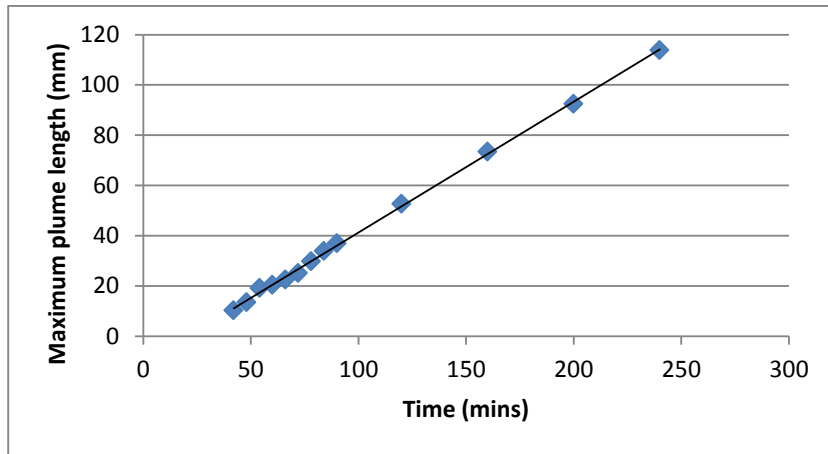maximum, gives a similar linear relationship and onset time.

Fig. 3: Maximum plume length against time from experimental data.

3. Numerical Modelling

Having experimentally reproduced the transition from diffusion-dissolution to dissolution-convection, the next step was to simulate the process numerically. A very high resolution model of the Hele-Shaw cell was built in the TOUGH2 flow simulator [5] with the ECO2N fluid property module [6]. The mesh comprised a 2D grid of 35075 elements, 305 horizontally with a size of 2 mm and 115 vertically, 1 mm deep for the first 50 mm, 2 mm deep for the next 50 mm and 5 mm deep for the rest of the section. Laboratory pressure and temperature conditions were applied and the permeability was set at 2.5×10^{-9} m^2. This value was determined from the experimentally determined onset time using stability analysis [7-9].
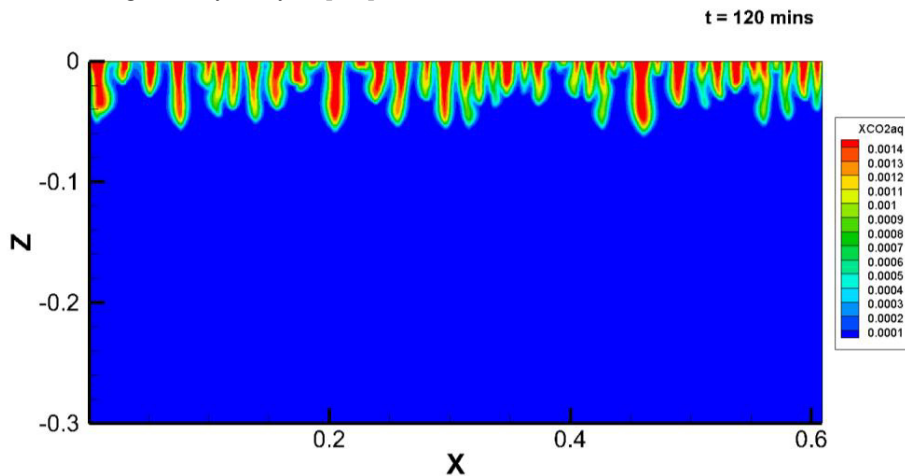

Fig. 4: Numerical simulation results for the homogeneous model after 120 minutes showing the progression of CO_2.

A sample of the numerical results (Fig. 4) shows a snapshot after 120 minutes, with warmer colours indicating higher concentrations of CO_2. Sinking plumes have formed at the top of the model, with a varied range of lengths up to a maximum of about 6 cm. An additional numerical model was created to represent a heterogeneous porous medium using random variations in the permeability for each cell. This is a technique widely used to account for natural heterogeneities [1, 2].

4. Results comparison

A comparison of experimental and numerical results at hourly intervals from 2 – 8 hours of CO_2 injection is shown in Fig. 5. The photographs of the Hele-Shaw cell have been processed by reduction to greyscale and a reversal of the tones to better highlight the presence of CO_2. Dissolved CO_2 (previously yellow) is dark against a light (previously purple) background. The observed and numerical plumes show a very good match for the whole recorded interval across the middle of the laboratory cell and the whole of the numerical domain (neglecting the preferential pathways down the cell edges). The plumes are generally quite long and thin, increasing in both length and width with time. The pH indicator in the cell detects dissolved CO_2 when it has reduced the pH by a unit. In comparison with the numerical results which show a more continuous range of concentrations, it may be more accurate to consider the higher concentrations (shown in red/yellow). When looking at only the red/yellow plumes given by the numerical results the match with the experimental results is remarkable (Fig. 5).

In the numerical model the plumes initially are very uniform in length and width but after 2 hours there are a range of lengths. Meanwhile in the experimental results gaps have formed between large plumes where small plumes have disappeared in preference to feeding the existing plumes which may contain preferential pathways. After 3 hours lobes have begun to form in the Hele-Shaw cell at the leading edge of the larger plumes, and in the numerical simulation on some of the smaller plumes. As time goes on these lobes become more significant and grow in size.

Similar experiments have been carried out in a Hele-Shaw cell but without a porous medium [3]; published results did not include comparisons at particular time steps and had a discrepancy on the rate of plume formation but the qualitative comparison was similar to the current study. Another study using a Hele-Shaw cell [4] presented results without a porous medium and found that the plumes developed faster in the experimental results than the numerical simulation.

Throughout the 8 hours displayed the length of the plumes is very comparable both for the larger plumes, and also, accounting for the abovementioned contouring/shading effects, for the smaller plumes (Fig. 5). A comparison of maximum plume length for the laboratory experiment with both numerical simulations (Fig. 6) shows very good agreement for the homogeneous simulation (as highlighted in Fig. 5), but not with the heterogeneous model where the permeability perturbations have increased the plume length. It is expected that additional model heterogeneities and triggers for plume formation would encourage an earlier onset time and this is confirmed by the comparison (Fig. 6).

The average plume spacing for the experimental and homogeneous numerical models was compared (Fig. 7). The discrepancy in this case is larger than it was for the plume length but a similar trend is shown for large times as, after the initial 2 hours, the spacings between plumes grow linearly with time.
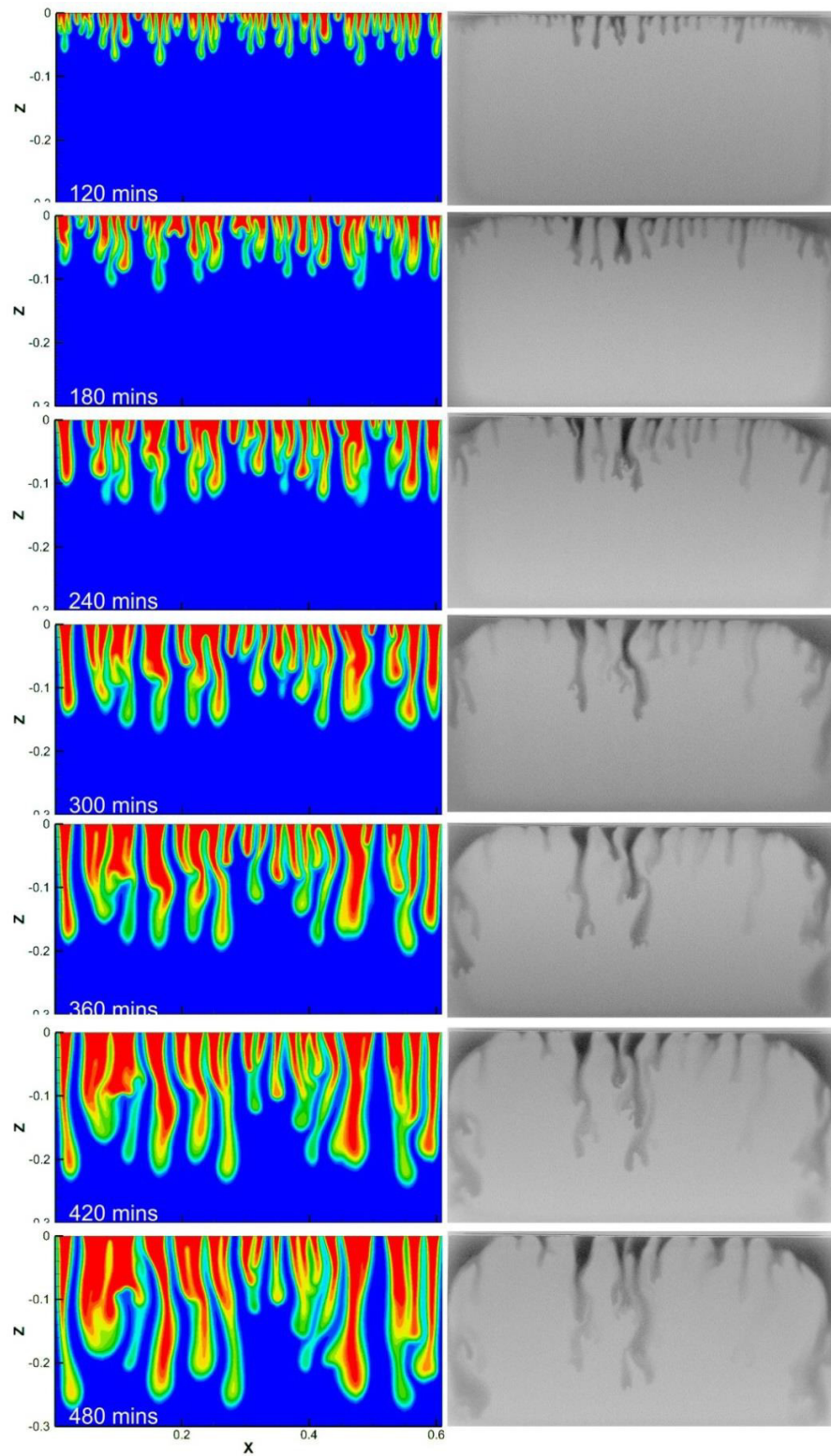
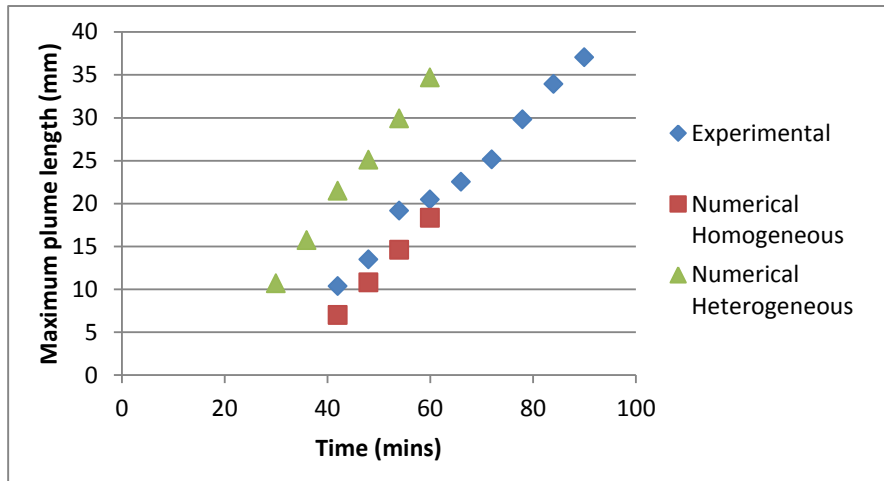Fig. 5: A comparison of numerical and experimental results after 2, 3, 4, 5, 6, 7 and 8 hours.

Fig. 6: A comparison of the maximum plume length against time for the experimental, homogeneous and heterogeneous models.
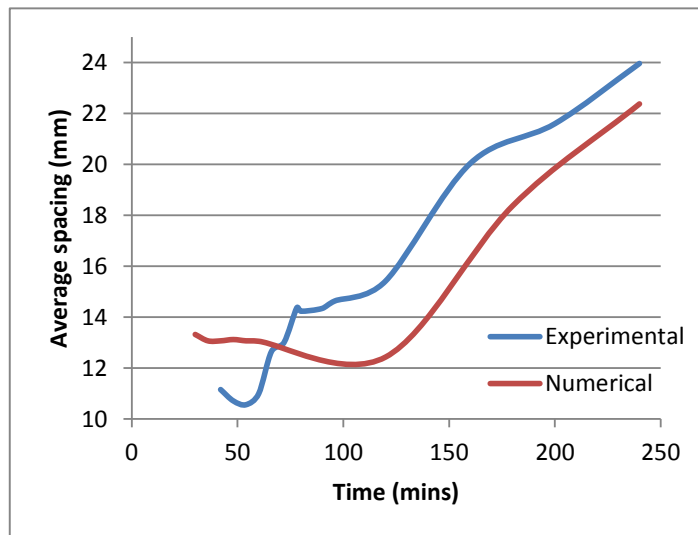

Fig. 7: The average measured plume spacing against time for the experimental and numerical results.

5. Conclusions

Away from the cell edges (where the experimental arrangement suffers from edge-effects), results of both the experiment and the numerical simulations are very comparable (Fig. 5). Plume temporal development is similar and plume dimensions in terms of length are closely comparable (Fig. 6). The spacing of the plumes is more complex, but the same overall trends are seen at later times (Fig. 7). The results suggest therefore that the numerical flow simulator is able to reproduce the critical process of transition from diffusion-dominated dissolution to convection-dominated dissolution in a porous medium on a laboratory scale. The triggering of instabilities in both homogeneous and heterogeneous numerical models has realistically replicated the observations.

In real reservoirs physical and chemical properties and overall timescales are significantly different from those in the laboratory and the issue of upscaling to a reservoir scale has the potential to magnify the discrepancies between numerical and experimental results, so there is still progress to be made in increasing confidence in numerical simulations over millennial time scales.

The results of this study have been reliable despite the fact that in the real case the instabilities are triggered by geological or physical heterogeneity, whereas in the simulator they are triggered by numerical rounding errors or arbitrary permeability perturbations. We are currently working on repeat experiments and simulations to improve the statistical robustness of our results.

Acknowledgements

References

[1] Lindeberg, E. and D. Wessel-Berg, Upscaling studies of diffusion induced convection in homogeneous and heterogeneous aquifers. 2011.
[2] Kong, X.-Z. and M.O. Saar, Numerical study of the effects of permeability heterogeneity on density-driven convective mixing during CO2 dissolution storage. International Journal of Greenhouse Gas Control, 2013. 19(0): p. 160-173.
[3] Faisal, T.F., S. Chevalier, and M. Sassi, Experimental and numerical studies of density driven natural convection in saturated porous media with application to CO2 geological storage. Energy Procedia, 2013. 37: p. 5323-5330.
[4] Kneafsey, T.J. and K. Pruess, Laboratory experiments and numerical simulation studies of convective enhanced carbon dioxide dissolution. Energy Procedia, 2011. 4: p. 5114-5121.
[5] Pruess, K., C. Oldenburg, and G. Moridis, TOUGH2 User Guide, version 2.0. Lawrence Berkeley National Laboratory Report LBNL-43134. 1999.
[6] Pruess, K., ECO2N: A TOUGH2 Fluid Property Module for Mixtures of Water, NaCl, and CO2. Lawrence Berkeley National Laboratory Report LBNL-57952. 2005.
[7] Grimstad, A.A. and E. Lindeberg, The feasibility of demonstrating diffusion induced convection in aquifers. 2007.
[8] Cheng, P., M. Bestehorn, and A. Firoozabadi, Effect of permeability anisotropy on buoyancy-driven flow for CO 2 sequestration in saline aquifers. Water Resources Research, 2012. 48(9).
[9] Wessel-Berg, D., On a linear stability problem related to underground CO2 storage. Journal of Applied Mathematics, 2009. 70: p. 1219-1238.